# Disappearance of static magnetic order and evolution of spin fluctuations in $Fe_{1+\delta}Se_xTe_{1-x}$

Zhijun Xu,[1,2] Jinsheng Wen,[1,3] Guangyong Xu,[1] Qing Jie,[1,3] Zhiwei Lin,[1] Qiang Li,[1] Songxue Chi,[4,5] D. K. Singh,[4,5] Genda Gu,[1] and J. M. Tranquada[1]

[1]*Condensed Matter Physics & Materials Science Department, Brookhaven National Laboratory, Upton, New York 11973, USA*

[2]*Department of Physics, City College of New York, New York, New York 10033, USA*

[3]*Department of Materials Science and Engineering, Stony Brook University, Stony Brook, New York 11794, USA*

[4]*NIST Center for Neutron Research, National Institute of Standards and Technology, Gaithersburg, Maryland 20899, USA*

[5]*Department of Materials Science and Engineering, University of Maryland, College Park, Maryland 20742, USA*

(Received 26 May 2010; revised manuscript received 26 August 2010; published 29 September 2010)

We report neutron-scattering studies on static magnetic orders and spin excitations in the Fe-based chalcogenide system $Fe_{1+\delta}Se_xTe_{1-x}$ with different Fe and Se compositions. Short-range static magnetic order with an in-plane wave vector near the (0.5,0) (using the two-Fe unit cell), together with strong low-energy magnetic excitations is found in all nonsuperconducting samples for Se doping up to 45%. When the static order disappears and bulk superconductivity emerges, the spectral weight of the magnetic excitations shifts to the region of reciprocal space near the in-plane wave vector (0.5, 0.5), corresponding to "collinear" spin correlations. Our results suggest that there is a strong correlation between superconductivity and the character of the magnetic order/fluctuations in this system. Excess Fe appears to be important for stabilizing the magnetic order that competes with superconductivity.

DOI: 10.1103/PhysRevB.82.104525 PACS number(s): 74.70.Xa, 75.25.−j, 75.30.Fv, 61.05.fg

## I. INTRODUCTION

Since the discovery of the first high-temperature superconductor in the 1980s, there has been a continuing effort to understand the origin of high-$T_c$ superconductivity. Studies on the cuprate systems seem to suggest that there is an intimate relationship between superconductivity and magnetism,[1–4] and recently this has been shown to be the case also for the newly discovered Fe-based superconductor families.[5–10] With nonsuperconducting parent compounds that have static antiferromagnetic (AF) order, charge doping in the Fe pnictides gradually suppresses the AF order and induces superconductivity for both the RFeAsO ("1111" system)[11–16] and $AFe_2As_2$ ("122" system) families.[17,18] In addition, a "spin resonance" has been observed in the 122 system[19–23] and in the 1111 system[24] by inelastic neutron scattering, showing a sharp increase in the magnetic scattering intensity at the "resonance" energy when the system goes into the superconducting phase. For the pnictides, both the static magnetic order in the parent compound and the resonance in the superconducting compounds occur around the in-plane wave vector (0.5,0.5) (using the two-Fe unit cell), suggesting a "collinear" or "C-type" AF structure [see Fig. 1(a)].[11,25,26]

The situation is slightly different in another Fe-based superconductor family, the iron chalcogenide $Fe_{1+\delta}Se_xTe_{1-x}$ (the "1:1" compound). Here the parent compound has a "bicollinear" or "E-type" AF order [see Fig. 1(b)],[25–29] modulated along the (0.5,0) in-plane direction. Furthermore, the substitution of Se for Te, which induces superconductivity, does not directly modify the density of electrons in the conduction bands. Despite these differences, the spin resonance observed in the superconducting compositions of this family has been found to occur at the same (0.5,0.5) in-plane wave vector,[29–37] as in the Fe pnictides,[19–23] but rotated 45° from the ordering wave vector of the parent $Fe_{1+\delta}$ Te compound. This suggests that the superconducting mechanism in the Fe pnictides and chalcogenides are likely to be quite similar. Nevertheless, there has also been a report implying that superconductivity can coexist with the bicollinear structure on the atomic scale.[38] Therefore, understanding how the magnetic structure (static or dynamic) evolves from the E-type bicollinear configuration of the parent compound to the C-type collinear configuration in the superconducting region in the 1:1 system is an important problem. There have been a number of theoretical studies[25,39] that provide some insight on this issue, but clearly a more systematic experimental study is highly desirable.

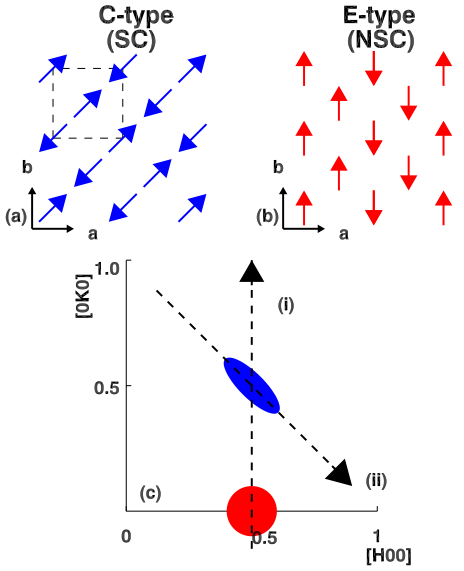


FIG. 1. (Color online) (a) Schematic of the collinear C-type AF spin structure with scattering intensities mainly around (0.5,0.5). The square shows a unit cell with two Fe atoms. (b) Schematic of the bicollinear E-type AF spin structure, which contribute mainly to scattering intensities near (0.5,0). (c) The schematic of the neutron-scattering measurements in the (*HK*0) zone. Dashed lines denote linear scans performed across (i) (0.5,0) and (ii) (0.5,0.5) in the text.

 

TABLE I. List of the $Fe_{1+\delta}Se_xTe_{1-x}$ samples used in our measurements, with their composition $(\delta,x)$, superconducting transition temperature $(T_c)$, room-temperature lattice parameters (from powder x-ray diffraction), crystal mass and ordered moment of Fe ion. The absolute value of ordered moment in NSC30 is undetermined because the measurements necessary for absolute normalization were not performed on that sample.

| Sample | $\delta$ | $x$ | $T_c$ (K) | $a$ (Å) | $c$ (Å) | Mass (g) | Moment per Fe ($\mu_B$) |
|---|---|---|---|---|---|---|---|
| SC30 | $0.00 \pm 0.03$ | 0.3 | 14 | 3.815 | 6.140 | 12.7 | 0.10 |
| NSC30[a] | $0.05 \pm 0.03$ | 0.3 | | 3.808 | 6.120 | 7.4 | Unknown |
| SC50[b] | $0.00 \pm 0.03$ | 0.5 | 14 | 3.811 | 6.129 | 9.0 | ~0 |
| NSC45 | $0.05 \pm 0.03$ | 0.45 | | 3.807 | 6.047 | 6.4 | 0.15 |

[a]Reference 28.
[b]Reference 32.

Previous work[29,35] reveals that while the high-energy magnetic excitation may not change much with Se doping, the low-energy spectral weight clearly shifts from around (0.5,0) to around (0.5,0.5). Nevertheless, it is less clear whether these changes are simply results of chemical substitution or related to the change in electronic states and emerging of superconductivity in the system. One approach to the problem is to study samples with similar Se doping but different superconducting properties.

In this paper, we present our work using neutron scattering to probe the magnetic order/fluctuations in a few samples from the 1:1 family for Se dopings ranging from 30% to 50% and with varying superconducting properties, the latter anticorrelated with excess Fe content. Our results suggest that static magnetic order exists in all nonsuperconducting samples. (Here, by nonsuperconducting we mean an absence of bulk superconductivity.) This order is short ranged and occurs at in-plane wave vectors **Q** of the type (0.5,0). For the fully superconducting samples, no static magnetic order is found. With the disappearance of static magnetic order, the associated low-energy magnetic excitations near (0.5,0) also go away, as one might expect. Magnetic excitations near (0.5,0.5) gradually become dominant as the material becomes more superconducting. While Se doping does play an essential role, it is clearly not the only determining factor regarding the superconductivity and the magnetic correlations. Samples with similar Se doping but differing in Fe content can have very different superconducting properties and corresponding magnetic structures/fluctuations. Our results clearly indicate that the static short-range magnetic order competes with and suppresses superconductivity. Superconductivity only appears when the system evolves toward fluctuating magnetic correlations characterized by $\mathbf{Q}=(0.5,0.5)$, which appears to be universal across all known Fe-based superconductor families. The situation has similarities to that in the high-$T_c$ cuprate systems where a resonance is also detected in the magnetic excitation spectrum for various cuprate families,[2–4,40,41] and static antiferromagnetic order suppresses bulk superconductivity. However, there is a clear difference between the two families: the local magnetic correlations in the cuprate system are always based on a G-type antiferromagnetic configuration,[25] even when spatial segregation occurs.[1,42–44] The versatility of spin configurations in the Fe-based superconductor families is therefore very different and extremely interesting.

## II. EXPERIMENT

The single-crystal samples used in the experiment were grown by a unidirectional solidification method. The samples, their compositions (nominal compositions, based on starting materials, with error bars for $\delta$ reflecting anticipated range of actual composition) and various characteristic properties are listed in Table I. The bulk susceptibility results in Fig. 2 were obtained using a superconducting quantum interference device (SQUID) magnetometer. Small well-cleaved samples were measured with vertical 5 Oe magnetic field applied perpendicular to the $a$-$b$ plane. From the magnetization measurements we can see that although both superconducting samples show evidence of diamagnetic response at around 14 K, SC50 is clearly better in quality as far as superconducting volume fraction is concerned. [Note that our zero-field-cooling (ZFC) measurements provide only an upper limit on superconducting volume fraction.] With a considerable portion of its bulk volume being nonsuperconducting, it is possible that there is phase separation in SC30.

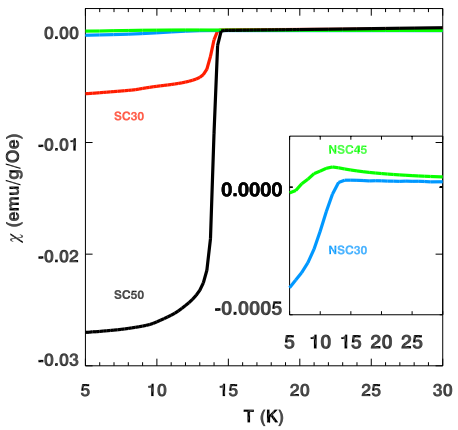


FIG. 2. (Color online) ZFC magnetization measurements by SQUID for SC30 (red), NSC30 (blue), NSC45 (green), and SC50 (black). The inset shows the same data from the nonsuperconducting samples with different scales.

In fact, when measuring different small pieces (~1 mm size) from the same SC30 sample, the superconducting volume can vary from ≲10% to ~80%, suggesting that the superconducting and nonsuperconducting phases could be macroscopically separated in this sample. The other samples, NSC30 and NSC45, are mostly nonsuperconducting, with no more than 1% of the volume giving a superconducting response.

Neutron-scattering experiments have been carried out on the triple-axis spectrometers SPINS (inelastic scattering measurements of magnetic excitations for SC30 and NSC30, and all elastic measurements for static magnetic order) and BT-7 (inelastic scattering measurements for SC50 and NSC45) located at the NIST Center for Neutron Research. We used horizontal beam collimations of guide-open-S-80′-240′ (S represents "sample") for the inelastic scattering measurements on SPINS with fixed final energy of 5 meV and a cooled Be filter after the sample to reduce higher-order neutrons; collimations of guide-80′-S-80′-240′ were used for the elastic measurements on SPINS with an additional Be filter before the sample. At BT7, we used beam collimations of open-50′-S-50′-240′ with fixed final energy of 14.7 meV and two pyrolytic graphite filters after the sample. The inelastic scattering measurements have been performed in the $(HK0)$ scattering plane, as indicated in Fig. 1(c). The data are described in reciprocal lattice units (r.l.u.) of $(a^*,b^*,c^*)=(2\pi/a,2\pi/b,2\pi/c)$. The elastic scattering measurements have been taken in the $(H0L)$ scattering plane instead, since the order in the parent compound occurs at half integer $L$ values (AF order along the $c$ axis). All data have been normalized into absolute units ($\mu_B^2$ eV$^{-1}$/Fe), using incoherent elastic scattering intensities from the samples.

## III. RESULTS AND DISCUSSION

The static long-range magnetic order in the parent compound $Fe_{1+\delta}Te$ appears near (0.5,0,0.5), corresponding to bicollinear E-type AF structure. With small Se doping, it has been observed that the order gradually becomes short ranged[28,29,45] and eventually disappears. Our results, however, suggest that the order can still remain with relatively large Se dopings (and excess Fe).

We performed elastic magnetic scattering measurements on all samples. For the SC50 sample, there is no elastic magnetic intensity at (0.5,0,0.5) while magnetic peaks are observed for all three other samples. In Fig. 3, we plot $H$ and $L$ scans through this AF wave vector for all samples at $T=4$ K. The measurements for NSC30, Figs. 3(d)–3(f), are from a previous report (see Fig. 2 of Ref. 28). Unfortunately, no absolute normalization was performed on that sample. The temperature dependence [Figs. 3(c) and 3(f)] for the NSC45, SC30, and NSC30 samples are very similar with the order gradually disappearing with heating. [For the SC50 sample, there is no elastic scattering intensity as shown in Fig. 3(a) for the whole temperature range measured.] The $H$ and $L$ scans performed at higher temperature ($T=34$ K) show no peak structure and are therefore used as backgrounds to be subtracted from the data. All peaks are much broader than the resolution, indicating the short-ranged nature of the magnetic order. The $H$ scans are peaked near but not exactly at $H=0.5$, similar to the results reported for NSC30 and another sample with 27% Se doping.[28] The $L$ scans, however, are qualitatively different. In previous reports on lower Se-doped 1:1 compounds,[28,34] the $L$-scan peaks around $L=0.5$, and intensity always goes to zero at $L=0$. In those cases, the magnetic order is always AF along the $L$ direction, whether short or long ranged. Here we see that after background subtraction, the scattering intensity at $L=0$ is still appreciable. This suggests that although the magnetic order still has a modulation along the $L$ direction, which peaks around $L=0.5$, favoring an AF configuration between Fe planes, the order has become much more two dimensional (2D). In the NSC45 sample, the three-dimensional (3D) long-range bicollinear AF magnetic order of the parent compound has not been entirely destroyed, but rather greatly reduced to 2D short-range order. The ordered moment per Fe is 0.15(4) $\mu_B$, much less than the value in the parent compound with long-range order.[27] It is, nevertheless, enough to destroy superconductivity. With this static magnetic order present, even with 45% Se doping, bulk superconductivity is still not achieved. In the SC30 sample, although the sample does show a superconducting phase transition at around 14 K, the superconducting volume is smaller than for the SC50 sample. The ordered moment is

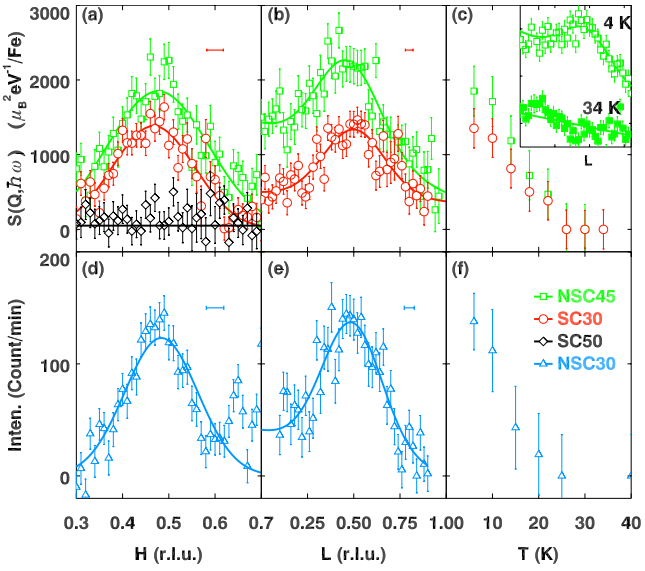


FIG. 3. (Color online) Elastic neutron-scattering measurements performed on SC30 (red circle), NSC30 (blue triangle), NSC45 (green square), and SC50 (black diamond) near (0.5,0,0.5). [(a) and (d)] Intensity profiles along [100] direction ($H$ scans) at $T=4$ K. [(b) and (e)] Scans along [001] direction ($L$ scans) at $T=4$ K. The horizontal bars represent the $H$ and $L$ resolutions at [(a) and (b)] SPINS and [(d) and (e)] BT-9. The solid lines are based on least-square fits to the data with single Gaussian peak and sloping background. (c) shows the magnetic peak intensity (from fitted Gaussian peak intensity) at (0.5,0,0.5) vs temperature. Corresponding scans measured at $T=34$ K are used as background and have been subtracted from all the data shown. The inset in (c) shows the 4 K (open) and 34 K (close) raw data used in (b) for NSC45. [(d)–(f)] Data from Ref. 28. The error bars represent the square root of the number of counts.

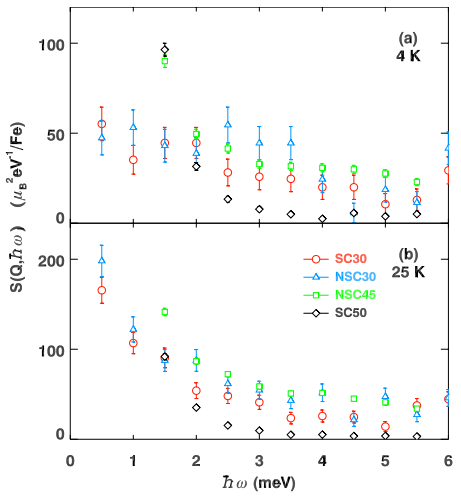


FIG. 4. (Color online) Constant-$Q$ scans at (0.5,0,0) taken at (a) 4 K (1.5 K for SC30 and NSC30) and (b) 25 K. A background, determined from constant-energy scans as in Fig. 5 has been subtracted from all data sets. The error bars correspond to the square root of the number of counts.

about 0.10(1) $\mu_B$/Fe, smaller than that in the NSC45 sample, indicating that this order may be coming from only part of the sample.

With the tendency toward developing static short-range magnetic order in the nonsuperconducting samples, it is natural to expect to see magnetic excitation spectra around the (0.5,0) in-plane wave vector as well. Previous work has shown that the energy dispersion and intensity modulation along the $L$ direction for magnetic excitations in the 1:1 compound is small.[30,34] We therefore chose to perform the inelastic scattering measurements in the ($HK$0) plane. In Figs. 4 and 5, we plot our results taken near (0.5,0,0). Figure 4 shows energy scans at (0.5,0,0) for $T$=4 and 25 K. Measurements for NSC45 and SC50 were taken on BT7 with a relatively coarse energy resolution [full width at half maximum (FWHM) ~ 1.7 meV] compared to those on SPINS (NSC30 and SC30, FWHM ~ 0.3 meV), and have a large, resolution-limited tail from scattering at $\hbar\omega$=0. Constant-energy scans at $\hbar\omega$=0.5, 2, and 5 meV [Figs 5(a)–5(f)] along the $K$ direction across (0.5,0,0) clearly show that for NSC30, SC30, and NSC45, there is significant spectral weight at low energies here. For both 30%-Se samples, where we have measurements with higher energy resolution, one can see that the intensity at $\hbar\omega$=0.5 meV increases on warming from 4 to 25 K. The increase is much less pronounced at $\hbar\omega$=5 meV. This behavior is likely due to a transfer of spectral weight from the elastic peak into low-energy channels when the static order dissolves with heating. For SC50, the low-energy spin excitations near (0.5,0,0) are weak and not strongly temperature dependent, which is consistent with the fact that there is no static order near (0.5,0) in this sample. The two small peaks near $K = \pm 0.5$ observed from samples SC30 and SC50 at $\hbar\omega$=5 meV, suggest that there is additional spectral weight developing near the (0.5,0.5) wave vector, corresponding to dynamic collinear spin correlations in the superconducting samples.

In Figs. 6 and 7, we show measurements near (0.5,0.5,0). For SC50, a clear resonance is observed when comparing the

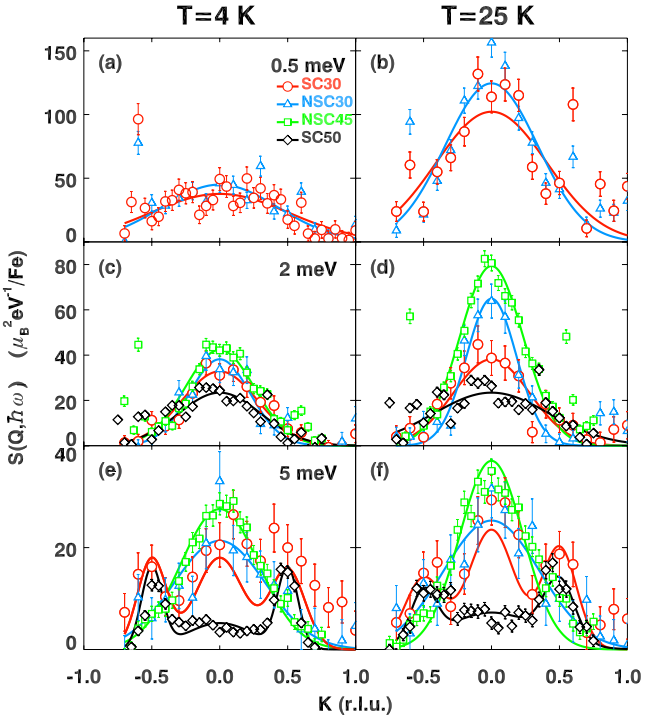


FIG. 5. (Color online) Magnetic excitations for $Fe_{1+\delta}Se_xTe_{1-x}$ measured around (0.5,0,0). The left and right columns show the magnetic peak profiles for 4 K (1.5 K for SC30 and NSC30) and 25 K, respectively. Constant-energy scans at (0.5, $K$, 0) [as shown by (i) in Fig. 1(c)] at [(a) and (b)] $\hbar\omega$=0.5 meV, [(c) and (d)] $\hbar\omega$ =2 meV, and [(e) and (f)] $\hbar\omega$=5 meV. The solid lines are based on least-square fits to the data with one main Gaussian peak at $K$ =0, plus sometimes two small Gaussian peaks at $K \pm 0.5$, which represent intensities from $Q$=(0.5,0.5), and a constant background. The fitted $K$-independent background has been subtracted from all data sets. The error bars correspond to the square root of the number of counts.

energy scans performed at 4 and 25 K (see Fig. 6). In Figs. 7(a)–7(f), constant-energy scans at $\hbar\omega$=5, 6.5, and 12 meV performed in the direction transverse to $\mathbf{Q}$=(0.5,0.5) are shown. Similar to SC50, but less pronounced, we can also see a resonance feature in SC30 in the scans of $\hbar\omega$=6.5 and 5 meV.

For the nonsuperconducting samples, there is no temperature effect observed for data taken between 4 and 25 K. For NSC30, we did a constant-energy scan near (0.5,0.5) only at $\hbar\omega$=6.5 meV, and the intensity is very low compared to either its own magnetic scattering near (0.5,0) or those from the other samples near (0.5,0.5). It is clear that the low-energy spin excitations are mostly focused around (0.5,0) for NSC30. The NSC45 sample has Se doping very close to SC50, and also very similar magnetic excitation spectrum near (0.5,0.5) compared to that from the latter in its normal state ($T$=25 K). However, with no superconducting transition, its spectrum at low temperature ($T$=4 K) does not differ much from that at $T$=25 K.

The implications of our results are very clear for NSC30 and SC50. For NSC30, a short-ranged static magnetic order is present at low temperature near (0.5,0), corresponding to a 3D bicollinear E-type spin structure. Its low-energy magnetic

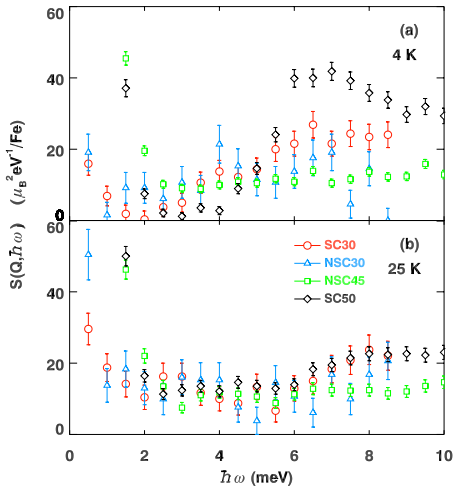


FIG. 6. (Color online) Constant-$Q$ scans at (0.5,0.5,0) taken at (a) 4 K (1.5 K for SC30 and NSC30) and (b) 25 K. A background, determined from constant-energy scans as in Fig. 7 has been subtracted from all data sets. The error bars corresponds to the square root of the number of counts.

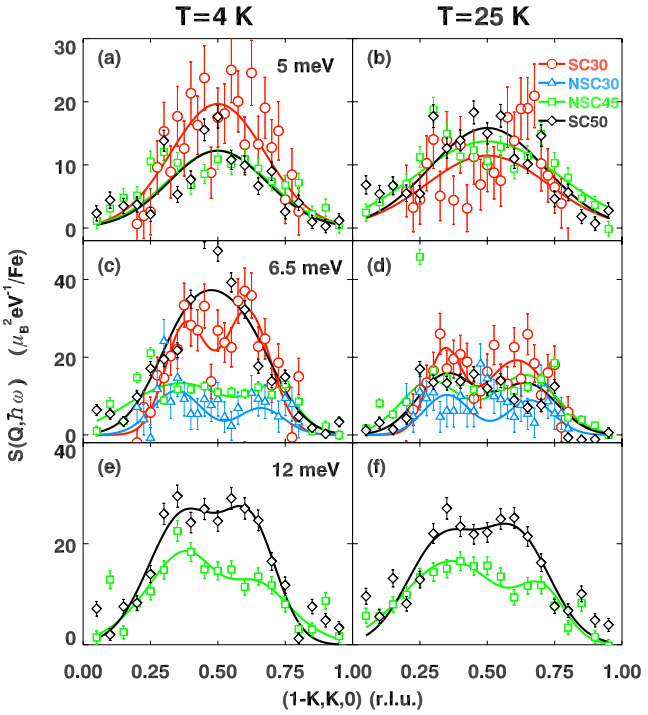


FIG. 7. (Color online) Magnetic excitations for $Fe_{1+\delta}Se_xTe_{1-x}$ measured around (0.5,0.5,0). The left and right columns show the magnetic peak profiles for 4 K (1.5 K for SC30 and NSC30) and 25 K, respectively. Constant-energy scans at (0.5,0.5,0), taken along the transverse direction [as shown by (ii) in Fig. 1(c)] at [(a) and (b)] $\hbar\omega$=5 meV, [(c) and (d)] $\hbar\omega$=6.5 meV, and [(e) and (f)] $\hbar\omega$=12 meV. The solid lines are based on least-square fits to the data with two Gaussian peaks and a constant background. The fitted constant background has been subtracted from all data sets. The error bars corresponds to the square root of the number of counts.

excitations are also focused near (0.5,0). With the static order present, no superconductivity is achieved in this sample. For the SC50 sample, there is no static order and the low-energy magnetic excitation spectrum is mostly shifted to the (0.5,0.5) region, corresponding to collinear C-type spin correlations. Similar to the situation in the 122 (Refs. 17 and 18) or 1111 system,[11–16] this collinear configuration without static order appears to favor superconductivity.

The results for NSC45 are more complicated. Here, with Se doping close to SC50, the magnetic excitations near the (0.5,0.5) point are rather similar to the superconductor, except that the resonance feature is missing. Apparently, having magnetic excitations near (0.5,0.5) associated with the collinear spin configuration is not sufficient for superconductivity to emerge. The presence of static 2D-like magnetic order is correlated with the suppression of superconductivity. Of course, the tetragonal crystal structure gives no energetic distinction between the ordering wave vectors (0.5,0) and (0.5,0.5) so that the magnetic configuration is relatively soft. We suggest that the greater concentration of Fe in this sample is the likely key to the magnetism at (0.5,0). It is possible that there is a mixed phase where the two types of magnetic correlations coexist on a microscopic level, similar to that of the mixed C-E phase in manganites,[46] as suggested in Ref. 25.

The case for SC30 is, in fact, quite intriguing. A 2D-like short-range static order exists at low temperature while low-energy magnetic excitations are found both around (0.5,0) and (0.5,0.5) with comparable spectral weight. Therefore, the magnetic excitation spectrum actually looks very similar to that in NSC45, yet there is bulk superconductivity in SC30 when the static magnetic order is also present. Compared to NSC45, the ratio of spectral weight near (0.5,0.5) to that near (0.5,0) is higher in SC30, indicating a larger volume of the sample favoring collinear spin correlations. The resonance occurs below $T_c$, showing an enhancement of spectral weight only near (0.5,0.5). This indicates that superconductivity only exists in the part of the sample with dynamic collinear spin correlations. Although it is conceivable that the static order and superconductivity could coexist in the same domains as suggested by previous muon spin spectroscopy ($\mu$SR) work,[38] it is also possible to have a system with macroscopic phase separation, where the volume of local collinear or bicollinear region is large enough to form separate domains. In this case, the features near (0.5,0) (elastic magnetic peak and low-energy magnetic excitations), and those near (0.5,0.5) come from different regions. This scenario would be consistent with the (varying) susceptibility results for different small pieces taken at different locations from this sample and agrees with results from all other samples where static magnetic order and superconductivity do not coexist locally.

Why would samples with similar Se content (e.g., NSC30 vs SC30, NSC45 vs SC50) show dramatically different behaviors? It is clear from previous work that the Fe content has a significant impact on the magnetism.[27,28] For example, higher Fe content in the parent compound can drive the order from commensurate to incommensurate[27] while its effect has been less clear for the superconducting region. It seems unlikely that the excess Fe atoms act simply as isolated magnetic moments that destroy the superconductivity, since our observations of variations in static magnetic order and low-

energy spin excitations cannot be explained in such a simple manner. Theoretically, it has been predicted that lowering the height of the chalcogen (Te/Se) positions can drive the 1:1 system from the bicollinear to the collinear spin configuration,[25,47] and Fe interstitials will certainly have an impact on Fe-Te/Se-Fe bond lengths and bond angles. There are several reports concerning the effect of excess Fe on the lattice parameters;[48–50] our results indicate that the lattice parameters *a* and *c* both decrease slightly with increased Fe content (holding Se constant), which does not appear to be entirely consistent with the trends reported by others. To make further progress on this issue, it will likely be necessary to characterize the microstructure associated with specific compositions.[48,51] For example, it has been suggested that the excess Fe atoms most likely reside around (0.25,0.25,0.7) (Ref. 26) which is on the opposite side to the Fe/Se sides in respect to the Fe planes. Since these Fe atoms are not ordered in any way, diffraction measurements are not very sensitive to their positions. Extended x-ray-absorption fine structure or x-ray/neutron pair-distribution function measurements may be more useful in order to probe the locations of these Fe atoms and their effect on the local structures.

## IV. SUMMARY

We have studied the relationship between superconductivity and the character of magnetic correlations in the 1:1 system. If the magnetic correlations in the system are characterized by $\mathbf{Q}=(0.5,0)$, which generally leads to static order, superconductivity is suppressed. We find that such correlations are enhanced in samples with excess Fe. Magnetic fluctuations at $\mathbf{Q}=(0.5,0.5)$, as found in other Fe-based superconductor families, are necessary, but not sufficient, for the emergence of bulk superconductivity. There are cases where magnetic correlations of both types coexist and compete. Overall, our results confirm that the nature of the magnetic correlations is critical to the occurrence of superconductivity in $Fe_{1+\delta}Se_xTe_{1-x}$.

## ACKNOWLEDGMENTS

We thank Weiguo Yin and Wei Ku for useful discussions. Work at Brookhaven is supported by the Office of Basic Energy Sciences, Division of Materials Science and Engineering, U.S. Department of Energy (DOE) under Contract No. DE-AC02-98CH10886. J.W. and Z.X. are supported by the Center for Emergent Superconductivity, an Energy Frontier Research Center funded by the U.S. DOE, Office of Basic Energy Sciences. The SPINS spectrometer at the NCNR is supported in part by the National Science Foundation under Agreement No. DMR-0454672.

[1] J. M. Tranquada, H. Woo, T. G. Perring, H. Goka, G. D. Gu, G. Xu, M. Fujita, and K. Yamada, Nature (London) **429**, 534 (2004).
[2] H. F. Fong, P. Bourges, Y. Sidis, L. P. Regnault, A. Ivanov, G. D. Gu, N. Koshizuka, and B. Keimer, Nature (London) **398**, 588 (1999).
[3] G. Xu, G. D. Gu, M. Hucker, B. Fauque, T. G. Perring, L. P. Regnault, and J. M. Tranquada, Nat. Phys. **5**, 642 (2009).
[4] H. A. Mook, P. Dai, S. M. Hayden, G. Aeppli, T. G. Perring, and F. Dogan, Nature (London) **395**, 580 (1998).
[5] Y. Kamihara, T. Watanabe, M. Hirano, and H. Hosono, J. Am. Chem. Soc. **130**, 3296 (2008).
[6] H. Takahashi, K. Igawa, K. Arii, Y. Kamihara, M. Hirano, and H. Hosono, Nature (London) **453**, 376 (2008).
[7] X. H. Chen, T. Wu, G. Wu, R. H. Liu, H. Chen, and D. F. Fang, Nature (London) **453**, 761 (2008).
[8] Z.-A. Ren, W. Lu, J. Yang, W. Yi, X,-L. Shen, Xheng-Cai, G.-C. Che, X.-L. Dong, L.-L. Sun, F. Zhou, and Z.-X. Zhao, Chin. Phys. Lett. **25**, 2385 (2008).
[9] F.-C. Hsu *et al.*, Proc. Natl. Acad. Sci. U.S.A. **105**, 14262 (2008).
[10] K.-W. Yeh *et al.*, EPL **84**, 37002 (2008).
[11] C. de la Cruz *et al.*, Nature (London) **453**, 899 (2008).
[12] J. Zhao *et al.*, Nature Mater. **7**, 953 (2008).
[13] Q. Huang, J. Zhao, J. W. Lynn, G. F. Chen, J. L. Luo, N. L. Wang, and P. Dai, Phys. Rev. B **78**, 054529 (2008).
[14] C.-H. Lee, A. Iyo, H. Eisaki, H. Kito, M. T. Fernandez-Diaz, T. Ito, K. Kihou, H. Matsuhata, M. Braden, and K. Yamada, J. Phys. Soc. Jpn. **77**, 083704 (2008).
[15] J. Zhao *et al.*, Phys. Rev. B **78**, 132504 (2008).
[16] Y. Qiu *et al.*, Phys. Rev. B **78**, 052508 (2008).
[17] J. Zhao, D. T. Adroja, D.-X. Yao, R. Bewley, S. Li, X. F. Wang, G. Wu, X. H. Chen, J. Hu, and P. Dai, Nat. Phys. **5**, 555 (2009).
[18] H. Chen *et al.*, EPL **85**, 17006 (2009).
[19] A. D. Christianson *et al.*, Nature (London) **456**, 930 (2008).
[20] M. D. Lumsden *et al.*, Phys. Rev. Lett. **102**, 107005 (2009).
[21] S. Chi *et al.*, Phys. Rev. Lett. **102**, 107006 (2009).
[22] S. Li, Y. Chen, S. Chang, J. W. Lynn, L. Li, Y. Luo, G. Cao, Z. Xu, and P. Dai, Phys. Rev. B **79**, 174527 (2009).
[23] D. S. Inosov *et al.*, Nat. Phys. **6**, 178 (2010).
[24] S. Wakimoto, K. Kodama, M. Ishikado, M. Matsuda, R. Kajimoto, M. Arai, K. Kakurai, F. Esaka, A. Iyo, H. Kito, H. Eisaki, and S. ichi Shamoto, J. Phys. Soc. Jpn. **79**, 074715 (2010).
[25] W.—G. Yin, C.-C.Lee, and W. Ku, Phys. Rev. Lett. **105**, 107004 (2010).
[26] S. Li *et al.*, Phys. Rev. B **79**, 054503 (2009).
[27] W. Bao *et al.*, Phys. Rev. Lett. **102**, 247001 (2009).
[28] J. Wen, G. Xu, Z. Xu, Z. W. Lin, Q. Li, W. Ratcliff, G. Gu, and J. M. Tranquada, Phys. Rev. B **80**, 104506 (2009).
[29] M. D. Lumsden *et al.*, Nat. Phys. **6**, 182 (2010).
[30] Y. Qiu *et al.*, Phys. Rev. Lett. **103**, 067008 (2009).
[31] H. A. Mook, M. D. Lumsden, A. D. Christianson, S. E. Nagler, B. C. Sales, R. Jin, M. A. McGuire, A. S. Sefat, D. Mandrus, T. Egami, and C. dela Cruz, Phys. Rev. Lett. **104**, 187002 (2010).
[32] J. Wen, G. Xu, Z. Xu, Z. W. Lin, Q. Li, Y. Chen, S. Chi, G. Gu, and J. M. Tranquada, Phys. Rev. B **81**, 100513(R) (2010).
[33] D. N. Argyriou *et al.*, Phys. Rev. B **81**, 220503 (2010).
[34] S.-H. Lee, G. Xu, W. Ku, J. S. Wen, C. C. Lee, N. Katayama, Z.

J. Xu, S. Ji, Z. W. Lin, G. D. Gu, H.-B. Yang, P. D. Johnson, Z.-H. Pan, T. Valla, M. Fujita, T. J. Sato, S. Chang, K. Yamada, and J. M. Tranquada, Phys. Rev. B **81**, 220502 (2010).

[35] T. J. Liu, J. Hu, B. Qian, D. Fobes, Z. Q. Mao, W. Bao, M. Reehuis, S. A. J. Kimber, K. Prokeš, S. Matas, D. N. Argyriou, A. Hiess, A. Rotaru, H. Pham, L. Spinu, Y. Qiu, V. Thampy, A. T. Savici, J. A. Rodriguez, and C. Broholm, Nature Mater. **9**, 718 (2010).

[36] S. Li, C. Zhang, M. Wang, H. Luo, E. Faulhaber, A. Schneidewind, J. Hu, T. Xiang, and P. Dai, arXiv:1001.1505 (unpublished).

[37] W. Bao, A. Savici, G. Granroth, C. Broholm, K. Habicht, Y. Qiu, J. Hu, T. Liu, and Z. Mao, arXiv:1002.1617 (unpublished).

[38] R. Khasanov *et al.*, Phys. Rev. B **80**, 140511(R) (2009).

[39] C. Fang, B. A. Bernevig, and J. Hu, EPL **86**, 67005 (2009).

[40] H. F. Fong, B. Keimer, D. L. Milius, and I. A. Aksay, Phys. Rev. Lett. **78**, 713 (1997).

[41] P. Dai, M. Yethiraj, H. A. Mook, T. B. Lindemer, and F. Dogan, Phys. Rev. Lett. **77**, 5425 (1996).

[42] J. M. Tranquada, B. J. Sternlieb, J. D. Axe, Y. Nakamura, and S. Uchida, Nature (London) **375**, 561 (1995).

[43] S. A. Kivelson, I. P. Bindloss, E. Fradkin, V. Oganesyan, J. M. Tranquada, A. Kapitulnik, and C. Howald, Rev. Mod. Phys. **75**, 1201 (2003).

[44] M. Fujita, H. Goka, K. Yamada, J. M. Tranquada, and L. P. Regnault, Phys. Rev. B **70**, 104517 (2004).

[45] N. Katayama, S. Ji, D. Louca, S. Lee, M. Fujita, T. Sato, J. Wen, Z. Xu, G. Gu, G. Xu, Z. Lin, M. Enoki, S. Chang, K. Yamada, and J. Tranquada, arXiv:1003.4525 (unpublished).

[46] T. Hotta, M. Moraghebi, A. Feiguin, A. Moreo, S. Yunoki, and E. Dagotto, Phys. Rev. Lett. **90**, 247203 (2003).

[47] C.-Y. Moon and H. J. Choi, Phys. Rev. Lett. **104**, 057003 (2010).

[48] T. M. McQueen, A. J. Williams, P. W. Stephens, J. Tao, Y. Zhu, V. Ksenofontov, F. Casper, C. Felser, and R. J. Cava, Phys. Rev. Lett. **103**, 057002 (2009).

[49] T. M. McQueen *et al.*, Phys. Rev. B **79**, 014522 (2009).

[50] R. Viennoisa, E. Gianninia, D. Marela, and R. Cerny, J. Solid State Chem. **183**, 769 (2010).

[51] R. Hu, E. S. Bozin, J. B. Warren, and C. Petrovic, Phys. Rev. B **80**, 214514 (2009).